DOI : 10.5958/2277-8934.2020.00027.2 *Vol 27 No 2, p 185-192*

DEOXYURIDINE 5-MONOPHOSPHATE (dUMP) METABOLISING ENZYME AND THE BIFUNCTIONAL DIHYDROFOLATE REDUCTASE-THYMIDYLATE SYNTHASE IN CAMELS AND *Trypanosoma evansi*

Mahmoud Kandeel[1,2,*] and Abdulla Al-Taher[1]

[1]Department of Biomedical Sciences, College of Veterinary Medicine, King Faisal University, Alahsa, 31982, Saudi Arabia
[2]Department of Pharmacology, Faculty of Veterinary Medicine, Kafrelsheikh University, Kafrelsheikh, 35255, Egypt

ABSTRACT

Bifunctional protein can be used as a drug target as it proves a classical difference between the host and parasite structures that can be used as a drug target. In this study, the metabolic pathways of deoxyuridine 5-monophosphate (dUMP) were compared in camel and the blood parasite *Trypanosoma evansi*. *T. evansi* shares similar profile with camel pathways but with predicted inability to degrade dUMP to uridine and devoid of dCTP deamination to yield dUMP. In the enzyme set of dUMP metabolism, thymidylate synthase was raised as a bifunctional enzyme in *T. evansi* with dihydrofolate reductase-thymidylate synthase (DHFR-TS) domains content, compared to a single TS domain in camels enzyme. Specific targeting of DHFR-TS in *T. evansi* is expected to yield specific anti-trypanosomal drugs.

Key words: Camel, DHFR-TS, dUTP, thymidylate synthase, *Trypanosoma evansi*

Computational techniques have largely enhanced drug discovery process by target identification and validation. It had been used to provide valuable knowledge about molecular targets in pathogens (Alnazawi *et al,* 2017; Kandeel *et al,* 2019a; Kandeel *et al,* 2019 in press; Kandeel *et al,* 2019b; Mahmoud *et al,* 2019). This process depends on comparison of genome sequences of the host and its pathogens. The sequence of camel genome was recently published (Jirimutu *et al,* 2012). This will give a new era in camel related research by defining the host spots in genome and proteome of camel and its pathogens against which drugs can be designed. Recently, we provided some interesting differences in the metabolic pathways of pyrimidines in camel and *T. evansi* (Kandeel and Al-Taher, 2020a; Kandeel and Al-Taher, 2020b; Kandeel *et al,* 2020).

In this study, enzymes of dUMP metabolism were compared in camels and the blood protozoan, *T. evansi*. In this respect, the KEGG maps were used to set up the enzymes set (Kanehisa *et al,* 2007; Kanehisa *et al,* 2016; Ogata *et al,* 1998). The bioinformatics tools were used to assess the standard enzymes in camel and *T. evansi*. Finally, differences in metabolic enzymes were highlighted and evaluated for vulnerability to be a drug target.

Materials and Methods

Retrieval of genomic data

Collection of genomic data was carried out by extracting the information from the gene database (http://www.genedb.org) (Hertz-Fowler *et al,* 2004), Kinetoplastom genome resources (http://tritrypdb.org/tritrypdb/), protein and genome databases at (http://www.ncbi.nlm.nih.gov) and the Arabian camel genome project (http://www.camel.kacst.edu.sa).

Searching homologues Protein sequence homologues were searched using the NCBI BLAST (Basic Local Alignment Search Tool) (Madden, 2013) or PSI-BLAST (Position- Specific Iterated-BLAST) servers (http://blast.ncbi.nlm.nih.gov/Blast.cgi) searching against the non redundant (nr) database, with filtering of low complexity regions.

Multiple sequence alignment programme for proteins and construction of phylogenetic tree was carried out using the tools available at (https://www.ebi.ac.uk/Tools/msa/clustalo/) (Sievers and Higgins, 2014). Multiple sequence alignment program (ClustalW2) was used to calculate the best match of the selected sequences. The resultant alignment was used to generate a phylogenic tree, which is visualised by Dendroscope phylogenic tree viewer (Huson *et al,* 2007) or CLC genomics workbench (Sequencing, 2011).

SEND REPRINT REQUEST TO MAHMOUD KANDEEL email: mkandeel@kfu.edu.sa

Putative domains were searched by the domain prediction programme available at (http://www.ncbi.nlm.nih.gov/Structure/cdd/cdd.shtml) (Marchler-Bauer *et al,* 2005). The genomic and molecular information was obtained from Kyoto Encyclopedia of Genes and Genomes (http://www.genome.jp/kegg/).

Proteomic and genomic tools ExPASy Proteomics tools (http://us.expasy.org/tools/) (Gasteiger *et al,* 2003) and tools available at the website of the European Bioinformatics Institute (http://www.ebi.ac.uk/Tools/) (Labarga *et al,* 2007) was also used for analysis of nucleotide and gene sequences. The protein parameters including the molecular weight, theoretical pI, amino acid composition, atomic composition, extinction coefficient, estimated half-life, instability index, aliphatic index and grand average of hydropathicity was searched at (http://us.expasy.org/tools/protparam.html). Protein sequences of target genes was analysed for data such as pI, extinction coefficient and MW for the tagged protein sequence by PROTParam. PROSITE (http://www.expasy.org/proteomics/families__patterns_and_profiles) was used to search for patterns and profiles in the protein sequences of the target genes. The protein domains, families and functional sites was searched at (http://prosite.expasy.org/).

Results and Discussion

Deoxyuridine-5′-monophosphate (dUMP) production process was proposed by 4 routes 1) dephosphorylation of deoxyuridine 5′-triphosphate by dUTP pyrophosphatase, 2) the dephosphorylation of deoxyuridine-5′-diphosphate by the actions of dTMP kinase 3) from deoxyuridine by the kinase activity of thymidine kinase 4) from dCTP by dCTP deaminase as shown in (Fig 1). In the catabolic direction, deoxyuridine was produced from dUMP by 5′-nucleotidase or 5′-deoxynucleotidase (Fig 1). In camel, the previous profile applied except for the absence of dCTP deamination to yield dUMP (Fig 2). *T. evansi* was found to be devoid of dCTP deamination and 5′-nucleotidase (Fig 3). Thus, dUMP was not converted to deoxyuridine. The summary of all enzymes in deoxyuridine pathways and the predicted enzymes in camels and *T. evansi* are provided in Tables 1-3.

Thymidylate synthase

Thymidylate synthase (EC 2.1.1.45; dTMP synthase), is a methyltransferase enzyme also called thymidylate synthetase; methylenetetrahydrofolate: dUMP C-methyltransferase; TMP synthetase. It acts on one-carbon moieties, as it catalyses methylation of dUMP with 5, 10-methylenetetrahydrofolate (methyl donor), creating dTMP and dihydrofolate (Slavik and Slavikova, 1980). Parasites, *Crithidia fasciculata, Crithidia oncopelti*, and a number of trypanosomatids (*Trypanosoma brucei, Trypanosoma congolense, Trypanosoma lewisi* and *Trypanosoma cruzi*) were able to synthesise several thymidylate synthases (TS). The trypanosotamid enzyme was inactivated by Mg^{2+}, was extensively more sensitive to mercaptoethanol, had elevated noticeable Km values for substrate (dUMP) and cofactor (tetrahydrofolate), had a greater obvious molecular weight and was significantly more sensitive to inhibition by suramin. Therefore, it is a promising target for chemotherapeutic agents, either on its own or in combination with a dihydrofolate reductase inhibitor (Chalabi and Gutteridge, 1977). Additionally, potency of inhibitory effects of antifolate drugs on targeted dual functionally dihydrofolate reductase-thymidylate synthase (DHFR-TS) that isolated from African trypanosomes, protozoan parasite causing both sleeping sickness in humans and nagana in cattle has been estimated. Thus, the most effective inhibitors for DHFR were methotrexate and trimetrexate, and for

Table 1. Enzymes involved in metabolic pathways of dUMP.

ID (E.C. number)	Definition (Enzyme name)
2.7.1.21	thymidine kinase
3.1.3.89	5′-deoxynucleotidase
3.1.3.5	5′-nucleotidase
3.5.4.30	dCTP deaminase (dUMP-forming)
3.6.1.23	dUTP diphosphatase; deoxyuridine-triphosphatase
2.7.4.9	dTMP kinase; thymidine monophosphate kinase
2.1.1.45	thymidylate synthase; dTMP synthase

Table 2. The expected enzymes involved in metabolic pathways of dUMP in camels.

ID (E.C. number)	Definition (Enzyme name)
2.7.1.21	thymidine kinase
3.1.3.5	5′-nucleotidase
3.6.1.23	dUTP diphosphatase; deoxyuridine-triphosphatase
2.1.1.45	thymidylate synthase; dTMP synthase

Table 3. The expected enzymes involved in metabolic pathways of dUMP in *Trypanosoma brucei*.

ID (E.C. number)	Definition (Enzyme name)
2.7.1.21	thymidine kinase
3.6.1.23	dUTP diphosphatase; deoxyuridine-triphosphatase
2.1.1.45	thymidylate synthase; dTMP synthase
2.7.4.9	dTMP kinase; thymidine monophosphate kinase

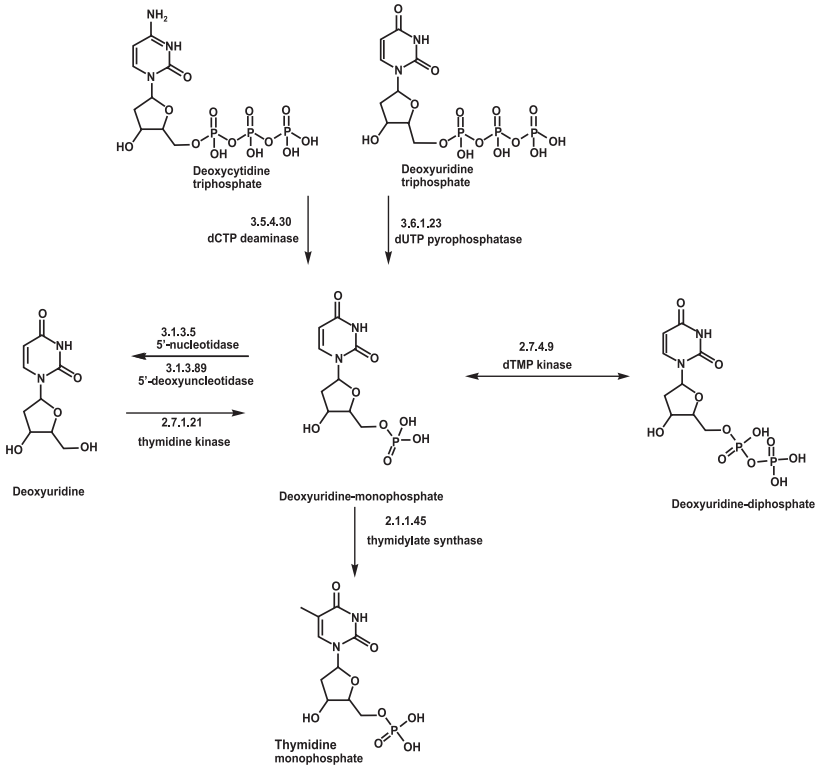

Fig 1. The proposed metabolic pathways of deoxyuridine monophosphate (dUMP).

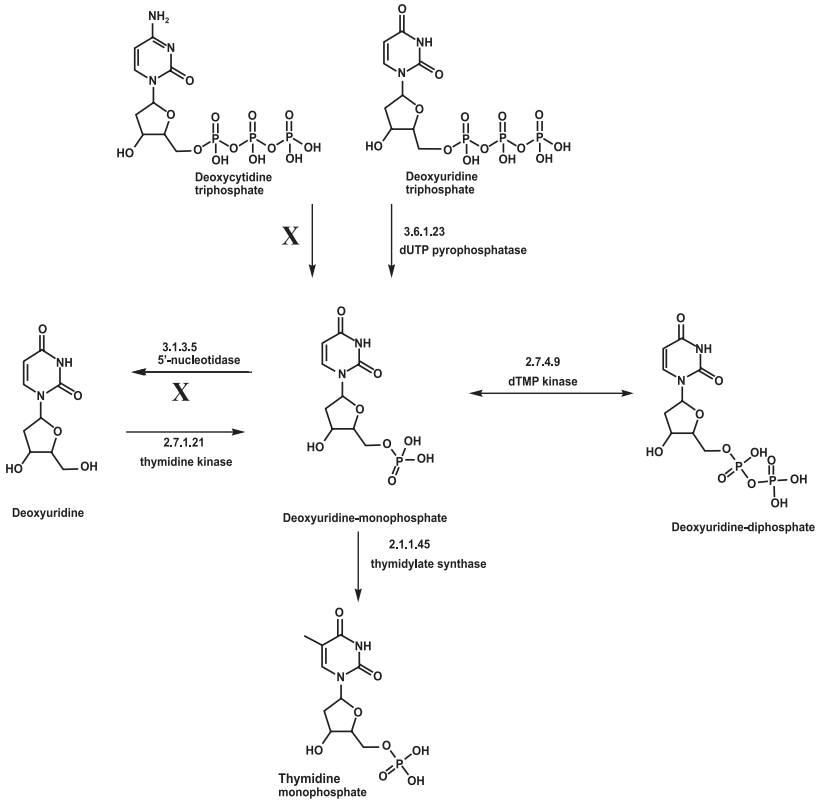

Fig 2. The proposed metabolic pathways of deoxyuridine monophosphate (dUMP) in camels.

thymidylate synthase were FdUMP and nolatrexed (Gibson *et al,* 2016).

Human and camel TS showed 77% similarity and 72 differences (Fig 4). This difference was attributed to the lack of 60 amino acids at the N-terminal of camel TS. In comparing the camel species, the dromedary and bactrian camels were 99.21% similar, while the similarity rate drops to 74.05 and 73.42% in comparing dromedary and bactrian camel with the feral camel. This was due to the lack of 58 amino acids at the N-terminal of dromedary and bactrian camels (Fig 5). Comparison of camel and *T. evansi* TS is provided in Fig 6. The camel protein was 253 amino acids, while the *T. evansi* TS is 527 amino acids in length forming 29.98% similarity and 369 differences. Motif and domain search using MotifFinder revealed the bifunctional dihydrofolate reductase-thymidylate synthase (DHFR-TS) was encoded by the *T. evansi* protein, while the camel enzyme encodes one thymidylate kinase domain (Fig 7).

The heat map of multiple comparison of TS sequences in several species showed 68.9-94.27% similarities among the selected vertebrates TS. Comparisons with protozoal and prokaryotes TS revealed low similarity rate in the range of 12-33.69% (Fig 8). The phylogenetics of camel and *T. evansi* TS is shown in (Fig 9). The *T. evansi* TS was related to the protozoal enzyme and highly related to the prokaryotic TS. The camel TS was related to the monofunctional eukaryotic thymidylate synthases.

The bifunctional DHFR-TS had been regarded as a promising antiprotozoal and anti-trypanosomal target (Gibson *et al,* 2016; Panecka-Hofman *et al,* 2017; Schormann *et al,* 2010; Senkovich *et al,* 2009; Valente *et al,* 2019). The present finding which highlights the differences between camel and *T. evansi* TS suggests using it as a drug target.

Molecular models of camel and human TS were requested from

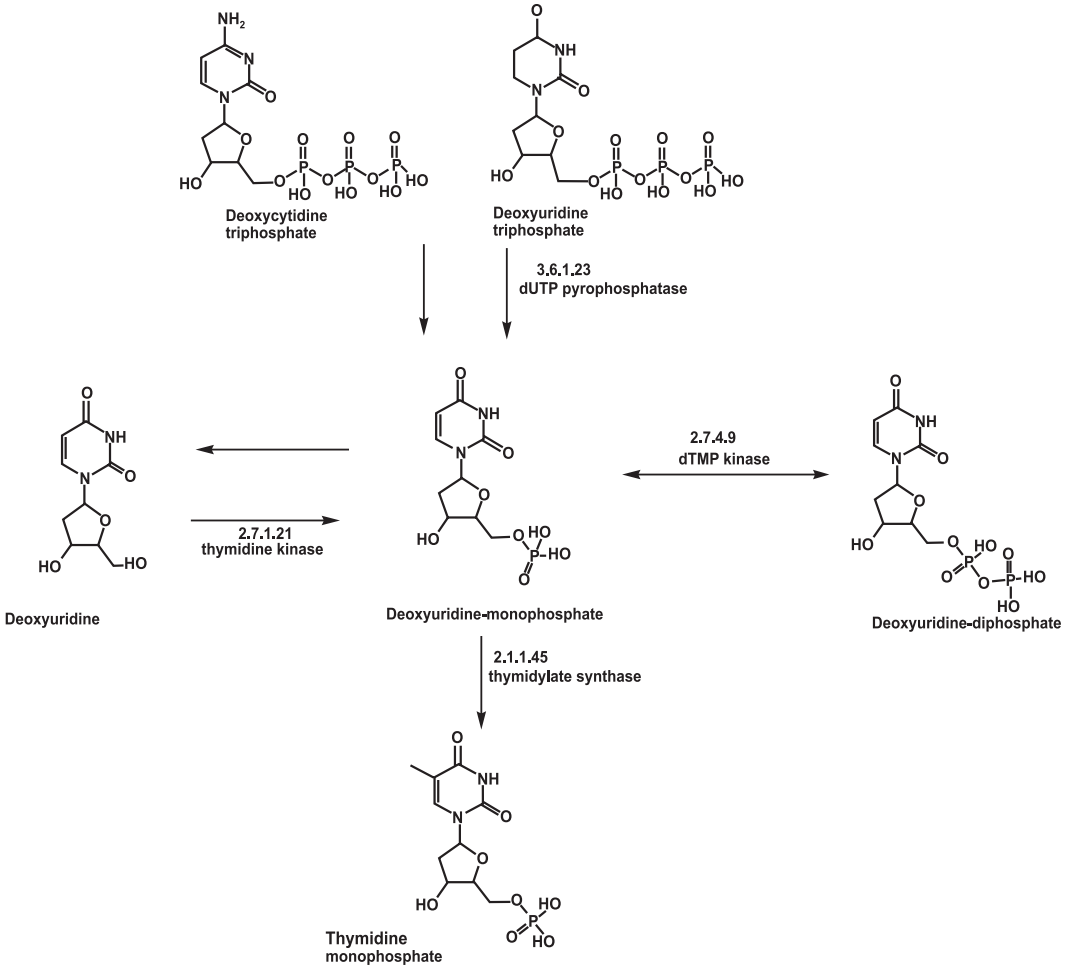

Fig 3. The proposed metabolic pathways of deoxyuridine monophosphate (dUMP) in *Trypanosoma brucei*.

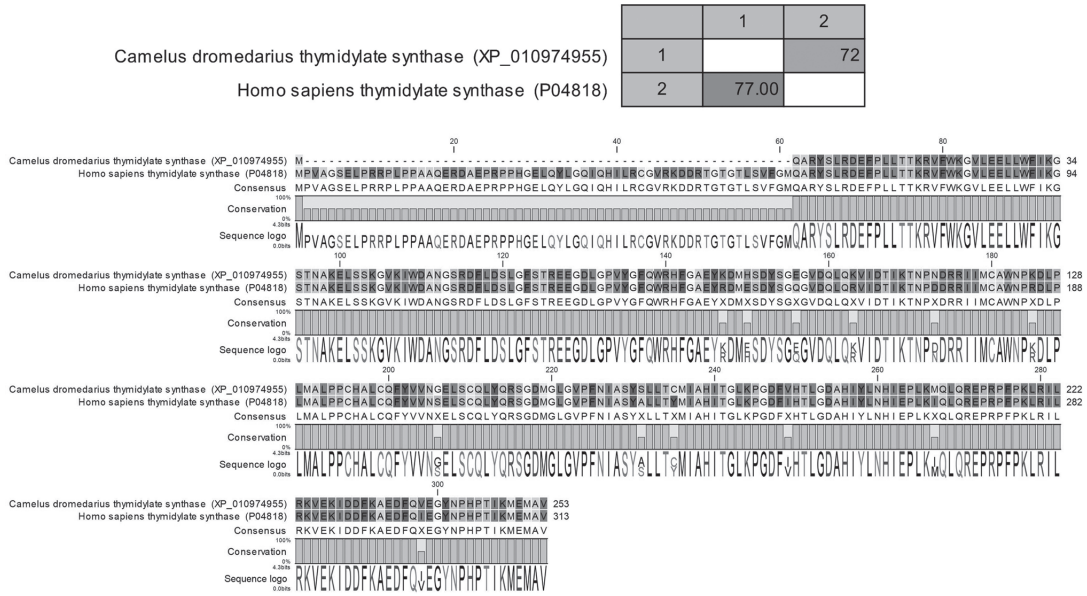

Fig 4. Multiple sequence alignment of dromedary camel and human thymidylate synthase. The upper panel represents sequence comparison statistics. The upper right diagonal region is explains the number of differences between two sequences, while the lower left diagonal region explains the per cent of identity between two sequences.

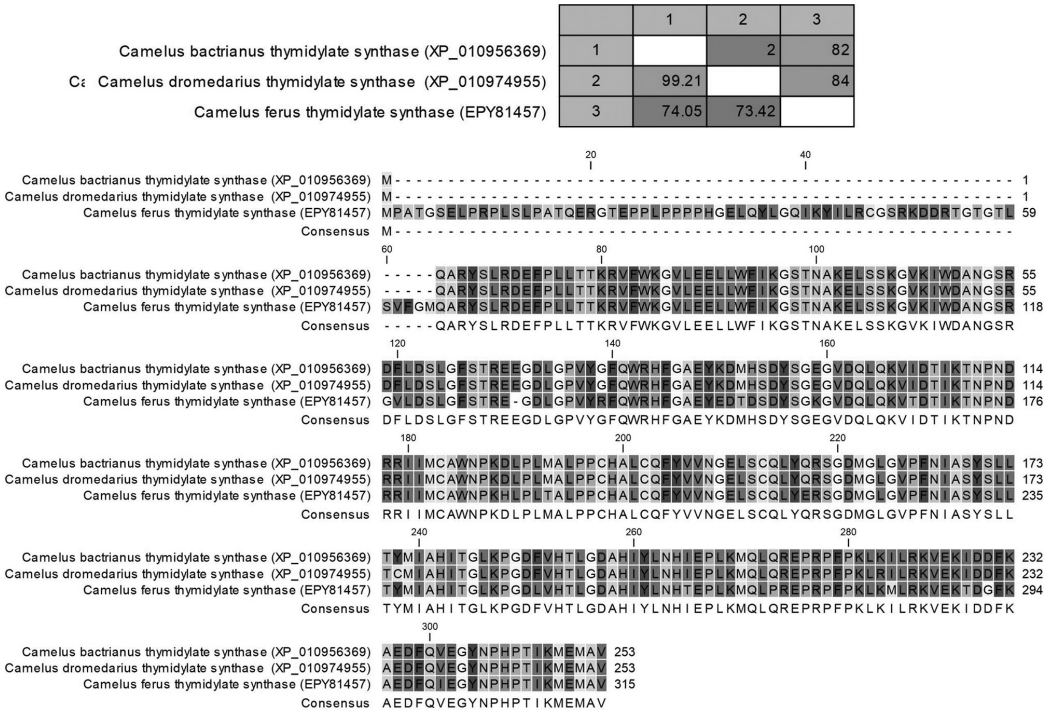

Fig 5. Multiple sequence alignment of dromedary, bactrian and feral camels thymidylate synthase. The upper panel represents sequence comparison statistics. The upper right diagonal region is explains the number of differences between two sequences, while the lower left diagonal region explains the per cent of identity between two sequences.

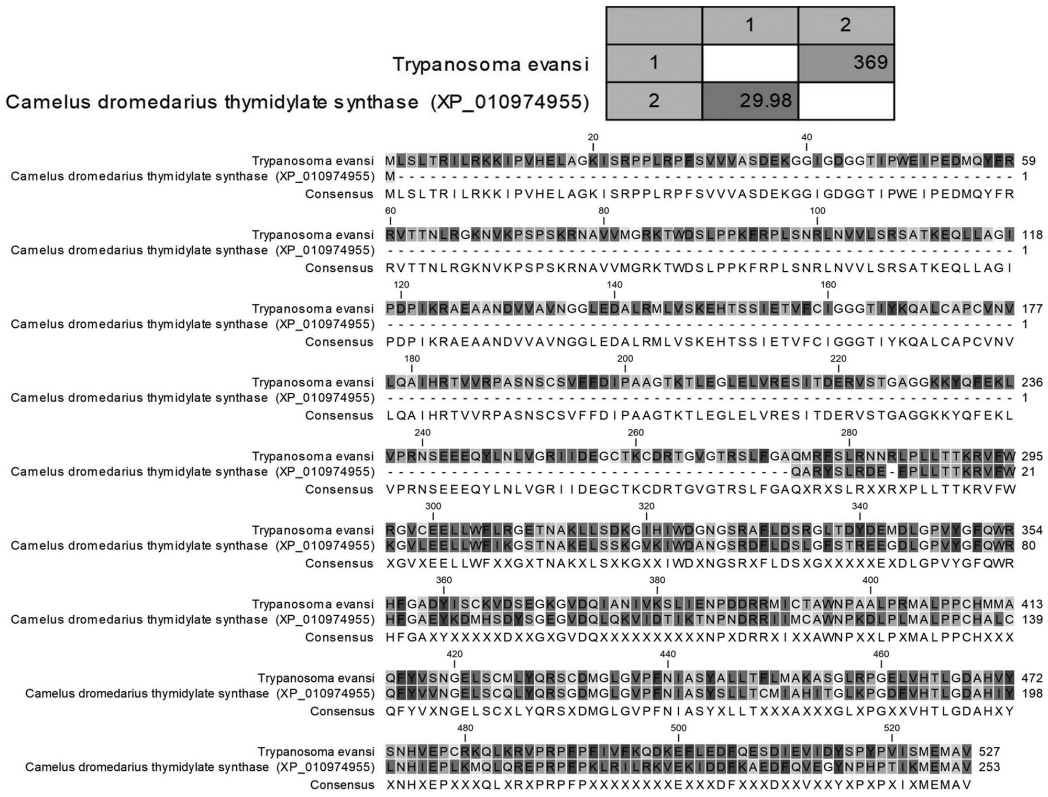

Fig 6. Multiple sequence alignment of dromedary camel and *Trypanosoma evansi* thymidylate synthase. The upper panel represents sequence comparison statistics. The upper right diagonal region is explains the number of differences between two sequences, while the lower left diagonal region explains the per cent of identity between two sequences.

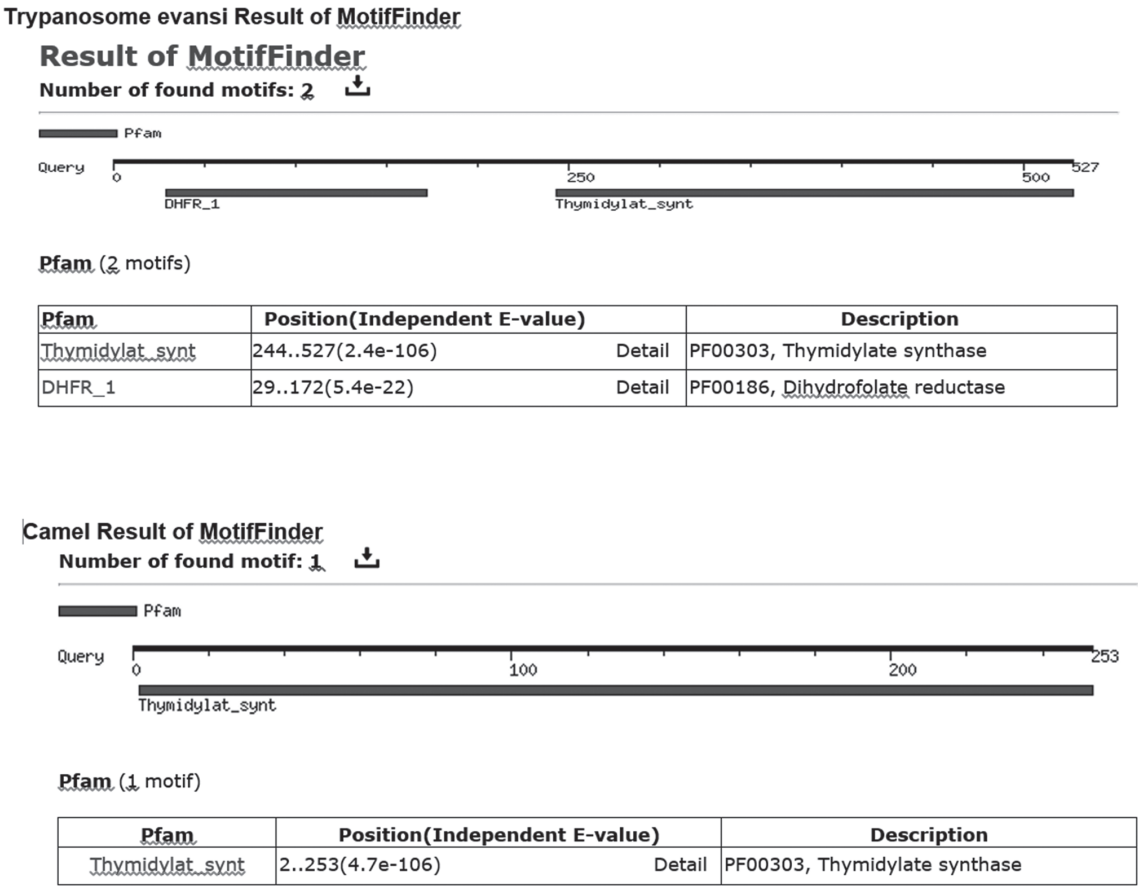

Fig 7. Motif and domain content of dromedary camel and *Trypanosoma evansi* thymidylate synthase.

	1	2	3	4	5	6	7	8	9	10	11	12	13	14	15	16	17	18	19	20	21	22	23	24	25	26
Bos taurus thymidylate synthase (NP_001032905)	1		39	44	40	41	42	38	47	47	47	39	101	101	56	62	249	249	257	332	116	104	92	103	113	144	188
Capra hircus thymidylate synthase (XP_005697121)	2	46		5	1	2	3	1	10	10	10	2	62	62	19	25	212	212	220	295	77	65	53	70	78	163	149
Oryctolagus cuniculus thymidylate synthase (XP_002713484)	3	66	23		4	5	4	6	9	9	9	7	57	57	18	22	217	217	225	300	72	60	48	65	73	158	144
Sus scrofa thymidylate synthase (NP_001230508)	4	60	18	18		1	2	2	11	11	11	3	61	61	20	26	213	213	221	296	76	64	52	69	77	162	148
Homo sapiens thymidylate synthase (P04818)	5	72	29	28	20		1	3	12	12	12	4	60	60	21	25	214	214	222	297	75	63	51	68	76	161	147
Equus caballus thymidylate synthase (XP_001492275)	6	70	27	26	24	33		4	13	13	13	5	59	59	22	24	215	215	223	298	74	62	50	67	75	160	146
Felis catus thymidylate synthase (XP_003995103)	7	69	27	33	26	33	35		9	9	9	1	63	63	18	24	211	211	219	294	78	66	54	71	79	164	150
Rattus norvegicus thymidylate synthase (NP_062052)	8	82	40	35	38	41	45	41		0	0	10	54	54	9	15	220	220	224	303	69	57	45	62	70	155	141
Rattus norvegicus thymidylate synthase (NP_062052)	9	82	40	35	38	41	45	41	0		0	10	54	54	9	15	220	220	224	303	69	57	45	62	70	155	141
Mus musculus thymidylate synthase (NP_067263)	10	81	39	33	37	42	44	41	9	0		10	54	54	9	15	220	220	224	303	69	57	45	62	70	155	141
Camelus ferus thymidylate synthase (EPY81457)	11	82	39	43	39	43	50	40	57	57	55		64	64	19	25	212	212	220	295	79	67	55	70	78	165	149
Camelus bactrianus thymidylate synthase (XP_010956369)	12	116	74	68	70	72	75	75	68	68	66	82		0	45	41	274	274	260	357	85	73	53	70	86	169	105
Camelus dromedarius thymidylate synthase (XP_010974955)	13	116	76	70	72	72	77	75	68	68	68	84	2		45	41	274	274	260	357	85	73	53	70	86	169	105
Gallus gallus thymidylate synthase (XP_015133440)	14	110	68	61	63	65	71	65	60	60	61	78	73	73		10	229	229	225	312	62	50	36	53	63	146	132
Ascaris suum thymidylate synthase (O96650)	15	159	121	116	121	123	120	122	116	116	115	129	118	118	111		233	233	219	316	54	42	30	47	55	140	126
Trypanosoma brucei brucei TREU927 dihydrofolate reductase-thymidylate synthase (XP_8461710	16	387	350	348	345	348	348	348	349	349	350	350	369	369	353	363		0	56	93	285	245	263	280	288	359	359
Trypanosoma evansi	17	387	350	348	345	348	348	348	349	349	350	350	369	369	353	363	1		56	93	285	245	263	280	288	359	359
Babesia bovis T2Bo dihydrofolate reductase_thymidilate synthase (XP_001609606)	18	401	362	363	361	361	358	362	363	363	362	372	363	362	353	365	365	365		107	269	243	247	266	274	345	345
Plasmodium falciparum Bifunctional dihydrofolate reductase-thymidylate (P13922)	19	487	449	452	445	449	445	448	448	448	447	457	465	466	448	449	431	431	356		366	326	344	363	371	442	442
Staphylococcus aureus thymidylate synthase (RYC35504)	20	250	210	202	208	211	206	214	201	201	199	222	198	199	194	201	436	435	411	516		74	62	65	99	168	166
Corynebacterium pseudotuberculosis thymidylate synthase (ATQ64965)	21	235	194	187	190	188	190	193	184	184	183	196	178	178	176	186	387	387	390	485	194		20	49	63	146	134
Salmonella enterica thymidylate synthase (ASE75162)	22	214	173	169	173	172	172	177	167	167	166	183	162	162	163	170	395	395	384	485	168	115		31	51	146	116
Pasteurella multocida thymidylate synthase (ATN16863)	23	276	239	231	237	234	233	238	230	230	230	242	214	214	222	228	452	452	444	541	242	224	199		64	133	127
Streptococcus pyogenes thymidylate synthase (QAZ36778)	24	299	261	254	259	259	256	262	255	255	255	263	241	241	246	245	473	473	461	557	271	233	217	244		131	129
Escherichia coli thymidylate synthase (RXP45233)	25	354	344	336	341	339	339	346	335	335	334	350	319	319	328	330	552	552	536	638	358	326	320	327	318		188
Clostridium tetani thymidylate synthase (SUY57245)	26	332	292	287	291	290	292	292	284	284	284	294	239	239	277	281	514	515	496	592	318	279	262	283	275	347	

Fig 8. Multiple sequence alignment of camel, *Trypanosoma evansi*, prokaryotes and eukaryotes thymidylate synthase. The upper panel represents sequence comparison statistics. The upper right diagonal region is explains the number of differences between two sequences, while the lower left diagonal region explains the per cent of identity between two sequences.

the Swiss-Model website (Waterhouse *et al,* 2018). The camel TS sequence was submitted to Swiss Model to predict its structure by automated model building tool. The website predicted the 3D camel structure based on the 3h9k pdf file which contains a homodimer of human TS. The best model was based on human TS with 100% sequence coverage and 61% similarity (Fig 10). The model of *T. evansi* TS showed the highest similarity with the bifunctional DHFR-TS. The highest similarity was with the structure of *T. cruzei* DHFR-TS (PDB ID 3irm) with coverage of 98% and similarity rate 0.52.

The bifunctional DHFR-TS in *T. evansi* is distinct from the camel enzyme. The structure and functional differences could put the enzyme as a hopeful target to develop specific drugs.

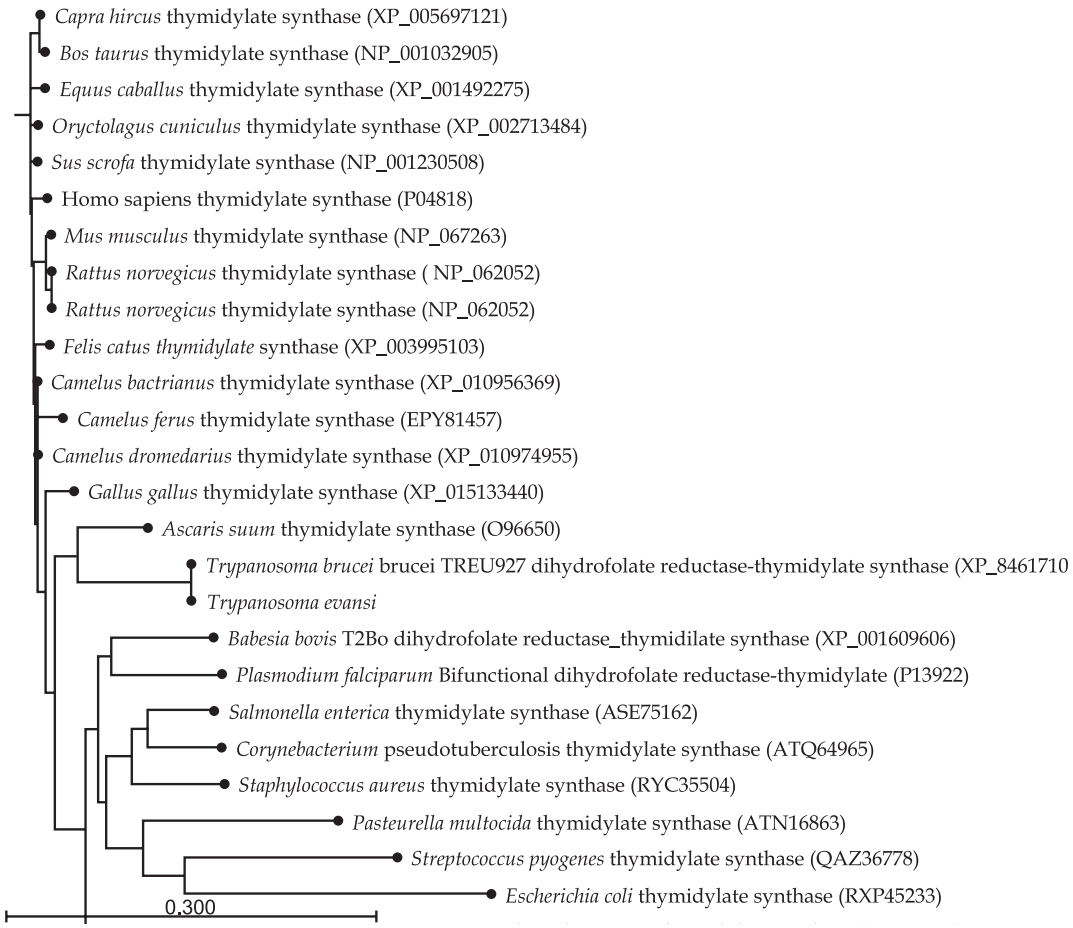

Fig 9. Phylogram of camel and *Trypanosoma evansi* bifunctional thymidylate synthase in relation to a set of prokaryotic and eukaryotic organisms.

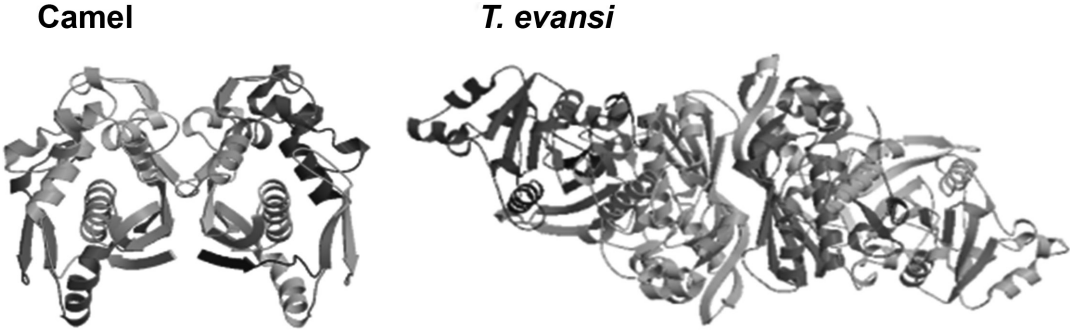

Fig 10. Molecular models of camel and *T. evansi* TS. The models were built by Swiss-Model server.

Acknowledgements

The authors acknowledge the financial support of this project by King Abdul-Aziz City for Science and Technology (KACST), Basic Research Programs, National Transformation Program, under Research and Development Grants Program for National Research Institutions and Centres (GPURC), Kingdom of Saudi Arabia (Grant No. 2-17-04-004-0001).

References

Alnazawi M, Altaher A and Kandeel M (2017). Comparative genomic analysis *MERS Cov* isolated from humans and camels with special reference to virus encoded helicase. Biological and Pharmaceutical Bulletin 40:1289-1298.

Chalabi KA and Gutteridge WE (1977). Presence and properties of thymidylate synthase in trypanosomatids. Biochim Biophys Acta 481:71-79.

Gasteiger E, Gattiker A, Hoogland C, Ivanyi I, Appel RD and Bairoch A (2003). ExPASy: the proteomics server for in-depth protein knowledge and analysis. Nucleic Acids Research 31:3784-3788.

Gibson MW, Dewar S, Ong HB, Sienkiewicz N and Fairlamb AH (2016). *Trypanosoma brucei* DHFR-TS Revisited: Characterisation of a bifunctional and highly unstable

recombinant dihydrofolate reductase-thymidylate synthase. PLoS Negl Trop Dis 10:e0004714.

Hertz-Fowler C, Peacock CS, Wood V, Aslett M, Kerhornou A, Mooney P, Tivey A, Berriman M, Hall N and Rutherford K (2004). GeneDB: a resource for prokaryotic and eukaryotic organisms. Nucleic Acids Research 32:D339-D343.

Huson DH, Richter DC, Rausch C, Dezulian T, Franz M and Rupp R (2007). Dendroscope: An interactive viewer for large phylogenetic trees. BMC bioinformatics 8:460.

Jirimutu, Wang Z, Ding G, Chen G, Sun Y, Sun Z, Zhang H, Wang L, Hasi S, Zhang Y, Li J, Shi Y, Xu Z, He C, Yu S, Li S, Zhang W, Batmunkh M, Ts B, Narenbatu, Unierhu, Bat-Ireedui S, Gao H, Baysgalan B, Li Q, Jia Z, Turigenbayila, Subudenggerile, Narenmanduhu, Wang Z, Wang J, Pan L, Chen Y, Ganerdene Y, Dabxilt, Erdemt, Altansha, Altansukh, Liu T, Cao M, Aruuntsever, Bayart, Hosblig, He F, Zha-ti A, Zheng G, Qiu F, Sun Z, Zhao L, Zhao W, Liu B, Li C, Chen Y, Tang X, Guo C, Liu W, Ming L, Temuulen, Cui A, Li Y, Gao J, Li J, Wurentaodi, Niu S, Sun T, Zhai Z, Zhang M, Chen C, Baldan T, Bayaer T, Li Y and Meng H (2012). Genome sequences of wild and domestic bactrian camels. Nat Commun 3:1202.

Kandeel M and Al-Taher A (2020a). Bioinformatics of uridine/deoxyuridine paths in *Trypanosoma evansi* revealed targeting uridine phosphorylase and cytidine deaminase. Journal of Camel Practice and Research 27:111-119.

Kandeel M and Al-Taher A (2020b). Uridine 5'-monophosphate (UMP) metabolising enzymes uracil phosphoribosyltransferase and orotidine-5'-phosphate decarboxylase/ump synthase in camels and *Trypanosoma evansi*. Journal of Camel Practice and Research 27:81-88.

Kandeel M, Altaher A and Alnazawi M (2019a). Molecular dynamics and inhibition of MERS CoV papain-like protease by small molecule imidazole and aminopurine derivatives. Letters in Drug Design and Discovery 16:584-591.

Kandeel M, Altaher A and Alnazawi M (2019). Molecular dynamics and inhibition of MERS CoV papain-like protease by small molecule imidazole and aminopurine derivatives. Letters in Drug Design and Discovery 16:1-8 (in press).

Kandeel M, Dalab A, Al-Shabebi A, Al-Taher A, Altaher Y and Abozahra M (2020). Uridine 5-triphosphate (UTP) metabolising enzymes nucleoside diphosphate kinase and cytidine triphosphate (CTP) synthase in camels and *Trypanosoma evansi*. Journal of Camel Practice and Research 27:61-68.

Kandeel M, Kitade Y, Al-Taher A and Al-Nazawi M (2019b). The structural basis of unique substrate recognition by *Plasmodium* thymidylate kinase: Molecular dynamics simulation and inhibitory studies. PLoS One 14:e0212065.

Kanehisa M, Araki M, Goto S, Hattori M, Hirakawa M, Itoh M, Katayama T, Kawashima S, Okuda S and Tokimatsu T (2007). KEGG for linking genomes to life and the environment. Nucleic Acids Research 36:D480-D484.

Kanehisa M, Furumichi M, Tanabe M, Sato Y and Morishima K (2016). KEGG: new perspectives on genomes, pathways, diseases and drugs. Nucleic Acids Research 45:D353-D361.

Labarga A, Valentin F, Anderson M and Lopez R (2007). Web services at the European bioinformatics institute. Nucleic Acids Research 35:W6-W11.

Madden T (2013). The BLAST sequence analysis tool. In: The NCBI Handbook (Internet) 2nd edition. National Centre for Biotechnology Information (US).

Mahmoud K, Kamal E, Wael E, Mahmoud F and Ibrahim G (2019). Species specificity and host affinity rather than tissue tropism controls codon usage pattern in respiratory mycoplasmosis. Journal of Camel Practice and Research 26:1-12.

Marchler-Bauer A, Anderson JB, Cherukuri PF, DeWeese-Scott C, Geer LY, Gwadz M, He S, Hurwitz DI, Jackson JD and Ke Z (2005). CDD: a conserved domain database for protein classification. Nucleic Acids Research 33:D192-D196.

Ogata H, Goto S, Fujibuchi W and Kanehisa M (1998). Computation with the KEGG pathway database. Biosystems 47:119-128.

Panecka-Hofman J, Pohner I, Spyrakis F, Zeppelin T, Di Pisa F, Dello Iacono L, Bonucci A, Quotadamo A, Venturelli A, Mangani S, Costi MP and Wade RC (2017). Comparative mapping of on-targets and off-targets for the discovery of anti-trypanosomatid folate pathway inhibitors. Biochim Biophys Acta Gen Subj 1861:3215-3230.

Schormann N, Velu SE, Murugesan S, Senkovich O, Walker K, Chenna BC, Shinkre B, Desai A and Chattopadhyay D (2010). Synthesis and characterisation of potent inhibitors of *Trypanosoma cruzi* dihydrofolate reductase. Bioorg Med Chem 18:4056-4066.

Senkovich O, Schormann N and Chattopadhyay D (2009). Structures of dihydrofolate reductase-thymidylate synthase of *Trypanosoma cruzi* in the folate-free state and in complex with two antifolate drugs, trimetrexate and methotrexate. Acta Crystallogr D Biol Crystallogr 65:704-716.

Sequencing H (2011). CLC Genomics Workbench. Workbench.

Sievers F and Higgins DG (2014). Clustal Omega, accurate alignment of very large numbers of sequences. In: Multiple Sequence Alignment Methods. Springer. pp 105-116.

Slavik K and Slavikova V (1980). Purification of thymidylate synthetase from enzyme-poor sources by affinity chromatography. Methods Enzymol 66:709-723.

Valente M, Vidal AE and Gonzalez-Pacanowska D (2019). Targeting Kinetoplastid and apicomplexan thymidylate biosynthesis as an antiprotozoal strategy. Curr Med Chem 26:4262-4279.

Waterhouse A, Bertoni M, Bienert S, Studer G, Tauriello G, Gumienny R, Heer FT, de Beer TAP, Rempfer C, Bordoli L, Lepore R and Schwede T (2018). SWISS-MODEL: homology modelling of protein structures and complexes. Nucleic Acids Res 46:W296-w303.